Anbar Journal of Engineering Science (AJES) **Vol. 12 , No. 2 (2021) , pp. 193 ~ 202**
P-ISSN: 1997-9428; E-ISSN: 2705-7440 DOI: https://doi.org/10.37649/aengs.2021.171187

Anbar Journal Of Engineering Science©

journal homepage: http:// www.uoanbar.edu.iq/Evaluate/

Unviersty of Anbar

Numerical Investigation of Hydraulic-Thermal Performance for a Double-Pipe Heat Exchanger Equipped with 45°-Helical Ribs

Ahmed K. Mashan , Waleed M. Abed, Mohammed A. Ahmed

Mechanical Engineering Department, College of Engineering, University of Anbar, Ramadi, Iraq

PAPER INFO

Paper history:
Received 8/9/2021
Revised 14/10/2021
Accepted 27/10/2021

Keywords:
CFD study, 45°-helical ribs, Double-pipe heat exchanger, Thermal performance, Heat transfer enhancement, Concentric annular gap.

ABSTRACT

In this paper, the hydraulic-thermal performance of a double-pipe heat exchanger equipped with 45°-helical ribs is numerically studied. The ribbed double-pipe heat exchanger is modelled using three heights (H = 0, 2.5, 3.75, 5 mm) of 45°-helical ribs. Two numbers (4-ribs and 8-ribs) of 45°-helical ribs are attached on the outer surface of the inner pipe of the counter-flow double-pipe heat exchanger and compared with a smooth double-pipe heat exchanger. Three-Dimensional computational fluid dynamics (CFD) model for a laminar forced annular flow is performed in order to study the characteristics of pressure drop and convective heat transfer. In addition, the influence of rib geometries and hydraulic flow behaviour on the thermal performance is systematically considered in the evaluations. The annular cold flow is investigated with the range of Reynolds numbers from 100 to 1000, with three heights of ribs at the same width (W = 2 mm) and inclined angles of (θ = 45°).

The results illustrate that the average Nusselt number and pressure drop increase with an increasing number of ribs, the height of ribs and Reynold number, while the friction factor decreases with increasing Reynolds numbers. The percentage of averaged Nusselt number enhancement for three rib heights (H = 2.5, 3.75 and 5 mm) at 4-ribs is (34%, 65% and 71%), respectively, While for 8-ribs the enhancement percentage is (48%, 87% and 133%) as compared with the smooth double-pipe heat exchanger at Re = 100. The best performance evaluation criteria of (PEC) at (8-ribs, and H = 5 mm) is 2.8 at Re = 750. The attached 45-helical ribs in the annulus path can generate kind of secondary flows, which enhance the fluid mixing operation between the hot surface of the annular gap and the cold fluid in the mid of the annulus, which lead to a high-temperature distribution. Increasing the height of 45°-helical ribs lead to an increase in the surface area subjecting to convective heat transfer.

.

* Corresponding author. : Ahmed K. Mashan; : ahmed.mashan@uoanbar.edu.iq ;

1. Introduction

Double-pipe heat exchangers are well-known for their widespread use in a variety of practical and engineering applications. Two concentric pipes are employed in a simple double-pipe heat exchanger, which is categorized into parallel and counter depending on the flow direction. In order to obtain the highest thermal performance of the heat exchanger's available surface area, the hot fluid flows in the inner pipe and the cold fluid flows in the annulus in the opposite flow direction, forming a "counter-flow heat exchanger". This arrangement is often used in a variety of industrial processes, including air coolers, waste heat recovery and conversion systems, and chemical process heating [1-3]. Recently, various studies have been done on the heat transfer enhancement of heat exchangers, Verma and Kumar [4] using helical-tape inserts for different pitch lengths of 50, 100, 150, 200, and 250 mm for 40 design points. This investigation was done for cold water at a constant velocity of 0.367 (m/s) and hot water in the velocity range of 0.127 to 0.577 (m/s). It can be seen that the heat transfer increases with a decrease in pitch length and friction factor decreased with increasing Reynolds number and Nusselt number. In 2017, El Maakoul et al. [5] examined the thermal-hydraulic performance of double-pipe heat exchangers fitted with helical baffles on the outer surface of the inner pipe. Convection heat transfer coefficient for a helical baffled annulus side was higher than convection heat transfer coefficient for a simple annulus side by about 5%, 17%, 30% and 45% on average, for a baffle spacing of 100 mm, 50 mm, 33.3 mm and 25 mm respectively. Other numerical investigations have been achieved by El Maakoul et al. [6], and the thermo-hydraulic performance of air-to-water double-pipe heat exchanger was studied with helical fins with the fins spacing range of (0.05–0.2 m) in the gas side of the annulus. The heat transfer surface area in the case of helical fins was 3% – 24% higher than that in the longitudinal fins case. The thermal performance of a double-pipe heat exchanger provided with twisted-tape inserting on the outer surface of the inner pipe was investigated by Scholar and Kumar [7]. Ten double-pipe heat exchangers in the counter-flow arrangement were constructed (with and without) with different height to pitch ratios and tested at different water flow rates in the annulus-side. The annulus average Nusselt number and friction factor increased with increasing mass flow rate. It was determined that the value of the friction factor lowered with an increase in Reynold numbers. Additionally, Soni and Khunt [8] numerically studied the design and development of DPHE with counter-flow by installing dimpled on the outer surface of the inner pipe at pitch length (40, 50, 60 mm) for evaluating convection heat transfer. When pitch among dimples increased the outlet temperature of the outer pipe side decreased and the temperature of the inner pipe side outlet increased so that the rate of heat transfer increased. Zhang et al. [9] studied the heat transfer characteristics of double-pipe heat exchanger joined with helical three-dimensional fins on the outer surface of the inner pipe. The maximum variation between the numerical results and the experimental data was approximately 6.3% for the Nusselt number and 9.8% for pressure drop, respectively. It was observed that the Nusselt number and pressure drop clearly increased with the Reynolds number increasing. Experimental and Numerical studies of double-tube heat exchangers were carried out by Eiamsa-ard et al. [10]. The principal objective of this work was to study the effect of modified twisted tapes in form of the regularly-spaced twisted tape with two different pitches to the width of the twisted tape (twist ratios) (y = 6.0 and 8.0) and three space ratios (($s = S / p_t$) = 1.0, 2.0, and 3.0) was compared with that of the full length twisted tapes, in order to find an optimum tradeoff between the enhanced heat transfer and the increased friction factor, full length twisted tapes (s = 0) consistently gave higher Nusselt numbers than regularly-spaced ones (s = 1.0, 2.0 and 3.0) and friction factors in the tubes with regularly-spaced twisted tapes inserts were consistently higher than that in the traditional tube.

In this work, a numerical simulation is accomplished for the laminar forced counter-flow using the ANSYS-FLUENT software in order to predict the hydraulic-thermal performance for a double-pipe heat exchanger equipped with 45°-helical ribs. These 45°-helical ribs of the double-pipe heat exchanger are modeled by changing the number (4-ribs and 8-ribs) and height (H = 2.5, 3.75, 5 mm) of the helical ribs for investigating thermal performance. In addition, the influences of geometric and hydraulic characteristics on thermal performance are systematically considered in the evaluations.

2. Numerical soluation

2.1. Physical Model

The purpose of this investigation is to study the thermal performance of a three-dimensional for a helically ribbed double-pipe heat exchanger (DPHE). The design was first drawn using SOLIDWORKS-14 by taking an angle of the ribs of 45° because it is the angle that achieves the highest amount of heat performance [11], and then it was transferred to the

ANSYS 19-R1 program.In addition, ribs, which include a change in the number and height of ribs, lead to changes in the velocity distribution and pressure along the annular gap of DPHE. Therefore, the amounts of the pressure drop and convective heat transfer will change. The configurations of ribbed DPHE are shown in Fig.1. The number of ribs used in this investigation is 4 and 8. Water (0.6 W/m.°Ǫ is selected as a working fluid in both concentric pipes and the material of the inner pipe is presumed aluminum (≈202 W/m.°Ǫ. Whereas it is assumed that the outer pipe is made of an insulating material, polythene for example, to achieve adiabatic boundary conditions. The cold water flows in the annular gap at Reynold number = (100 to 1000), while the hot water flowing in the inner pipe in a counter-flow direction. The height of ribs is changed of H = 0, 2.5, 3.75, 5 mm in order to achieve the ratio between the rib height and the annular gap (12.5 mm) as 0.2, 0.3, and 0.4 more geometry and properties details are listed in Table 1.

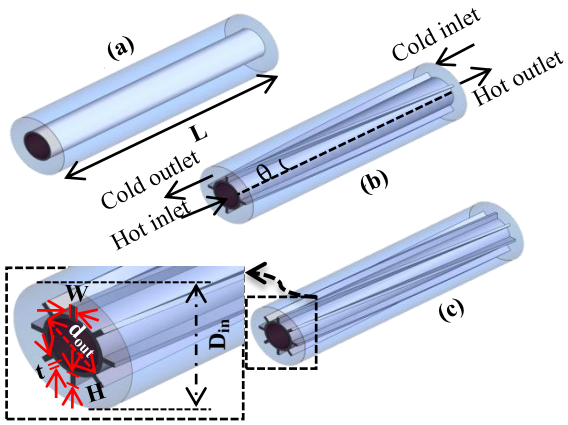

Figure 1. Physical geometry double-pipe heat exchanger for (a) smooth, (b) 4-ribs, and (c) 8-ribs.

Table 1. Structural model parameters

Material	Aluminum
The outer diameter of the inner pipe	25 mm
Thickness of inner pipe	2.5 mm
Inner diameter of outer pipe	50 mm
Length of DPHE	200 mm
Rib height	(0, 2.5, 3.75, 5) mm
Rib width	2 mm

2.2. Governing Equations

Working fluid (water) is assumed as an incompressible, steady-state and Newtonian fluid with constant thermo physical properties. In addition, the fluid flow occurs under laminar flow conditions, the maximum value of Reynolds number is (1000). The governing (continuity, momentum and energy) equations adopted in the current study can be expressed as [12].

Continuity Equation:

$$\left(\frac{1}{r}\frac{\partial(ru_r)}{\partial_r}+\frac{1}{r}\frac{\partial u_\emptyset}{\partial_\emptyset}+\frac{\partial u_z}{\partial_z}\right)=0 \quad (1)$$

Momentum equations in cylindrical coordinates are:

Radial-Momentum:

$$\left(u_r\frac{\partial u_r}{\partial_r}+\frac{u_\emptyset}{r}\frac{\partial u_r}{\partial_\emptyset}-\frac{{u_\emptyset}^2}{r}+u_z\frac{\partial u_r}{\partial_z}\right)=-\frac{\partial p}{\partial r}+$$

$$+\mu_{f_c}\left(\frac{1}{r}\frac{\partial}{\partial r}\left(r\frac{\partial u_r}{\partial r}\right)+\frac{1}{r^2}\frac{\partial^2 u_r}{\partial \emptyset^2}+\frac{\partial^2 u_r}{\partial z^2}-\frac{u_r}{r^2}-\frac{2}{r^2}\frac{\partial u_\emptyset}{\partial \emptyset}\right) \quad (2)$$

Tangential-Momentum:

$$\rho_{f_c}\left(u_r\frac{\partial u_\emptyset}{\partial_r}+\frac{u_\emptyset}{r}\frac{\partial u_\emptyset}{\partial\theta}+u_z\frac{\partial u_\emptyset}{\partial z}+\frac{u_r u_\theta}{r}\right)=-\frac{1}{r}\frac{\partial P}{\partial\theta}+$$

$$+\mu_{f_c}\left(\frac{1}{r}\frac{\partial}{\partial r}\left(r\frac{\partial u_\emptyset}{\partial r}\right)+\frac{1}{r^2}\frac{\partial^2 u_\emptyset}{\partial\emptyset^2}+\frac{\partial^2 u_\emptyset}{\partial z^2}-\frac{u_\emptyset}{r^2}+\frac{2}{r^2}\frac{\partial u_r}{\partial\emptyset}\right) \quad (3)$$

Axial-Momentum:

$$\rho_{f_c}\left(u_r\frac{\partial u_z}{\partial r}+\frac{u_\emptyset}{r}\frac{\partial u_z}{\partial\emptyset}+u_z\frac{\partial u_z}{\partial z}\right)=$$

$$-\frac{\partial P}{\partial z}+\mu_{f_c}\left(\frac{1}{r}\frac{\partial}{\partial r}\left(r\frac{\partial u_z}{\partial_r}\right)+\frac{1}{r^2}\frac{\partial^2 u_z}{\partial\emptyset^2}+\frac{\partial^2 u_z}{\partial z^2}\right) \quad (4)$$

Energy Equation:

$$\left(u_r\frac{\partial T}{\partial r}+\frac{u_\theta}{r}\frac{\partial T}{\partial\emptyset}+u_z\frac{\partial T}{\partial z}\right)=\alpha\left(\frac{1}{r}\frac{\partial}{\partial r}\left(r\frac{\partial T}{\partial r}\right)+\frac{1}{r^2}\frac{\partial^2 T}{\partial\emptyset^2}+\right.$$

$$\left.\frac{\partial^2 T}{\partial z^2}\right) \quad (5)$$

Where μ_{f_c} and ρ_{f_c} represent the dynamic viscosity and density of water, respectively. P represents the pressure, u represents the velocity vector, T is the local fluid temperature, and $\alpha_{f,c}$ is the thermal diffusivity.

2.3. Domain definition, mesh sensitivity and boundary conditions

Ribbed and smooth DPHE are modeled in this research. The traditional DPHE was simulated here for the purpose of comparison and the numerical model validation. The helical ribbed DPHE has different heights in the annulus side at the same width. The geometry was defined on the fluid domain (hot and cold water) and the solid domain was divided into 7 separate bodies. The computational domains were meshed with mixing hexahedral and tetrahedral meshes for both solid domain and fluid domain of the selected 4-ribs and 8-ribs DPHE as shown in Fig. 2. The orthogonal and skewness quality for the 4-ribs and 8-ribs DPHE were equal to (0.83 and 0.19) and (0.77 and 0.24), respectively.To ensure the accuracy of the numerical results, the mesh independent test was carried out for 4-ribs and 8-ribs DPHE to obtain optimization mesh. Five sets with the ele-

ment number varying from (0.77×106) to (2.16×10^6) at Re = 1000. It was found that the deviation in the averaged Nusselt numbers between 1.6 million and 1.38 million was less than 0.35% for 4-ribs DPHE, while the deviation in the averaged Nusselt numbers between 1.8 million and 1.5 million is less than 0.08% for 8-ribs DPHE as depicted in Fig. 3.

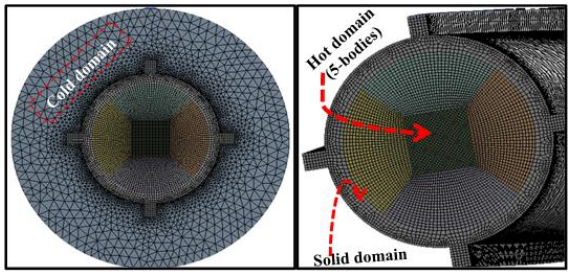

Figure 2. The suitable mesh generation for 4-ribs DPHE.

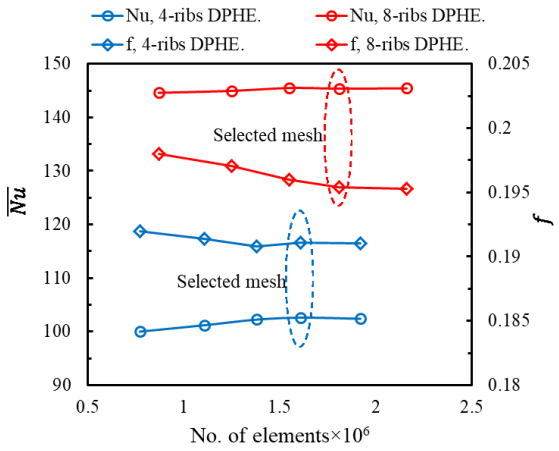

Figure 3. Showing grid independence test for 45°-helical ribs of double-pipe heat exchanger.

The boundary condition of no-slip was set for all the solid surfaces. The cold and hot water inlet were 27 and 70°C, respectiveliy, a uniform velocity (U_m) was applied at the inlet of the internal pipe and concentric annulus. The outlet of internal pipe and concentric annulus were employed ($P_{out} = P_{gage}$) at the value of ($P_{gage} = 0$) to avoid reversed flow. The program CFD-FLUENT was applied to determine the fluid flow and heat transfer in the computational domains. By using the finite-volume formulation and coupling methods algorithms, the governing equations were solved repeatedly. The second-order upwind scheme was adopted for the momentum and energy, the iterations continue until all of the computing processes residuals are indefinitely small (less than10^{-6}).

3. data reduction

The mean annulus side fluid velocity is defined by:

$$U_m = \frac{\dot{m}_{f_c}}{\rho_{f_c} A_c} \quad (6)$$

Where a $\dot{m}_{f_c}$ is the mass flow rate, ρ_{f_c} water density in the annulus side and A_c cross-section area of annulus.
Reynolds number can be calculated as the following formula [13]:

$$Re = \frac{\rho_{f_c} U_m D_h}{\mu_{f_c}} \quad (7)$$

Where μ_{f_c} the dynamic viscosity in the annulus side.

For the smooth annular pipe($D_h = D_{in} - d_{out}$), while for the ribbed annulus, the hydraulic diameter is [6]:

$$D_h = \frac{4[\frac{\pi}{4}({D_{in}}^2 - {d_{out}}^2) - NHW]}{N(2H+W) + \pi d_{out} - NW} \quad (8)$$

Where D_{in} represented the inner diameter of outer pipe, while D_{out} represented outer diameter of inner pipe.

Heat transfer rate of the annulus gap fluid (cold water):

$$Q_{f_c} = \dot{m}_{f_c} C_{p,f_c} (T_{b,out} - T_{b,in}) \quad (9)$$

Where $\dot{m}_{f_c}$ (kg/s) mass flow rate and $C_{p,f}$ (J/kg.°C) is specific heat of the fluid. The averaged Nusselt Number ($\overline{Nu}$) can be calculated as [14]:

$$\overline{Nu} = \frac{\bar{h} D_h}{k_{f_c}} \quad (10)$$

Where, $\bar{h}$ is the annulus side heat transfer coefficient. The penalty of pressure-drop and friction factor characteristics described in [13]:

$$f = 2\Delta P \times \frac{D_h}{\rho_{f_c} {U_m}^2 L} \quad (11)$$

Where, ($\Delta P = P_{in} - P_{out}$)
The thermal-hydraulic performance evaluation criterion (PEC) is a non-dimensional variable calculated as following [14]:

$$PEC = \left(\frac{\overline{Nu}_R}{\overline{Nu}_S} \Big/ \sqrt[3]{\frac{f_R}{f_S}}\right) \quad (12)$$

Where the subscript symbols R and S refer to the ribbed and smooth DPHE.

4. Results and Discussion

4.1. Numerical Model Validation

In order to confirm the numerical results, a comparison is done with experimental data using analytical relationships to evaluate pressure drop and heat transfer characteristics for ribbed DPHE. The range of mean velocity in the annulus gap was ranging from 0.0034 m/s to 0.034 m/s, in the same time the mean velocity of hot water in the inner pipe was varying from 0.0019 m/s to 0.019 m/s. The cold water inlet temperature was constant at 27 ℃and the hot water inlet temperature was set at 70 ℃ The max averaged Nusselt number of the annular gap has a relative deviation of 9.7% compared with Shah and London [15]. Table 2 represents the numerical data of friction factor-Reynolds number product (fRe), and $\overline{\mathrm{Nu}}$ is firstly compared with the data reported by Ref. [15] for concentric straight annular pipes. Flow in fully-developed and laminar in the concentric straight annular tubes with outer surface insulated (adiabatic) and the inner at (constant temperature, and heat flux) with aspect ratio (r*= 0.5).

Table 2. Showing comparison between the analytical solution of Shah and London [14] and present numerical data

Re	*f*.Re	Dev. (%)	$\overline{\mathrm{Nu}}$	Dev. (%)
constant temperature boundary condition				
100	23.19	2.634	5.291	7.823
500	24.32	3.720	5.4426	5.182
1000	23.45	1.529	5.291	7.824
Shah and London [15]	23.81	------	5.740	------
constant heat flux boundary condition				
100	24.33	2.239	6.3367	2.518
500	24.32	0.049	6.682	8.112
1000	24.31	2.144	6.7806	9.702
Shah and London [15]	23.8	------	6.1810	------

2.3. Domain definition, mesh sensitivity and boundary conditions

This section focuses on the study of thermal and hydraulic performance for the ribbed double-pipe heat exchangers with the variation of helical rib heights and number of ribs. The effect of height ribs is investigated for 4 and 8 helical rib numbers. The friction factors, Nusselt numbers and performance evaluation criterion are adopted for representing the characteristics of fluid flow and heat transfer within the ribbed double-pipe heat exchangers over a wide range of Reynolds numbers from 100 to 1000 and compared with smooth double-pipe heat exchanger.

4.2.1. Flow characteristics

The data of friction factor (f) versus Reynolds numbers for two the numbers of ribs and the numerical data of smooth DPHE is shown in Fig. 4. The values of friction factor dramatically decrease with rising Reynolds numbers. The values of friction factor increase with increasing number of ribs of DPHE. Fig. 5 shows the velocity contours of fluid flow at the cross-sectional planes (at three different locations

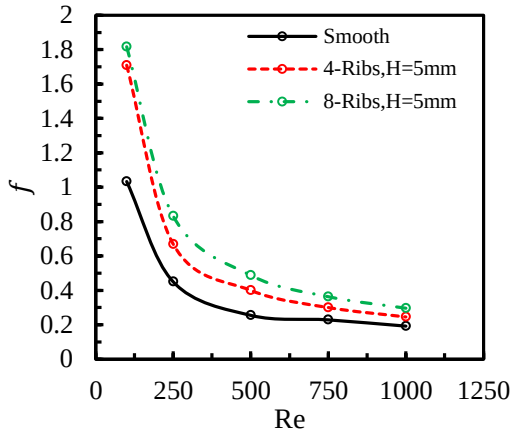

Figure 4. Variation of friction factor versus Reynolds numbers for both smooth and ribbed double-pipe heat exchangers.

along the annulus, 0L, 0.5L and L) and the axial plane direction within the ribbed annular gap as compared with smooth DPHE. In order to understand the behavior of fluid flow within the annular gap. Two numbers of longitudinal 45°-helical ribs (4 and 8) with the rib dimensions of H = 5 mm and W = 2 mm and Reynolds numbers of 100 and 1000 are numerically investigated. The existence of 45°-helical ribs along the axial flow direction supports the formation of hydraulic secondary flows in the main flow direction, the generated secondary flows are able to change the configuration of velocity stream from the ribbed pipe surface for improving fluid mixing, the velocities are distributed differently depending on the number of the ribs, and thickness hydraulic boundary layer, increase Reynold with helical ribs lead to more reduce in the hydrulic boundary layer thickness. At the Reynold number increasing (Re = 1000), the intensity of secondary flows over the ribs increases as the rib number increasing. The secondary flows created change in the velocity distribution pattern.

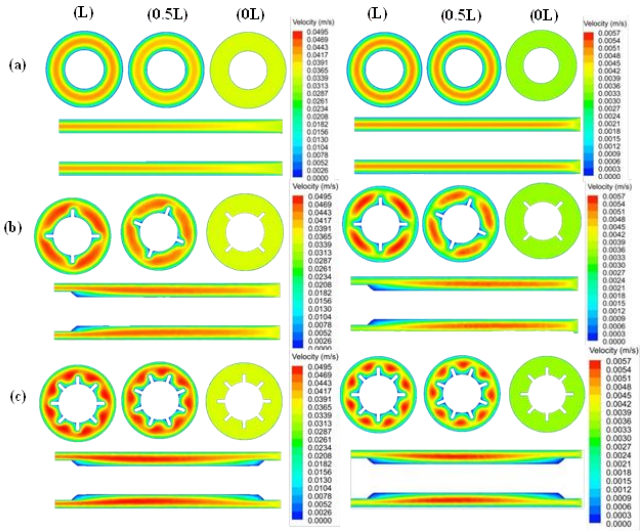

Figure 5. Velocity contours (left) at Re = 1000 and (right) at Re = 100 at (a) smooth, (b) (4-ribs, H= 5 mm) and, (c) (8-ribs, H= 5 mm).

4.2.2. Heat transfer characteristics

The averaged Nusselt number ($\overline{Nu}$) and outlet cold fluid temperature ($T_{b,out}$) versus Reynolds numbers for numerical results with three models according to the number of ribs can be shown in Fig. 6. ($T_{b,out}$) values will be decreased with increasing Reynold numbers, while the values of the ($\overline{Nu}$) increase with an increasing in the number of ribs due to the reduction in the thermal boundary layer thickness, for practical needs, the 45°-helical ribs are designed to reducing the thermal boundary layer thickness to increase the heat exchange.

Fig. 7 display the contours of temperature field in the axial annular plane direction and in the cross-sectional planes (at three different locations along the annulus) within the ribbed annular gap as compared with smooth DPHE, with (H= 5 mm and W= 2 mm) at *Re* = 100 and 1000. The generated secondary flows enhance fluid mixing between the hot fluid near the heated surface and the cold fluid in the mid of the annular gap, which leads to a high-temperature distribution. The intensity of temperature gradients increases with an increased number of helical ribs due to the increase of wetted surface area subjecting to convective heat transfer. The swirling flow is able to raise the rate of exchanged heat transfer. In (Fig .7-b and c) shows the difference along the length of the annulus for heat exchange, where the increase in heat exchange at the beginning of the annulus is high due to a decrease in the thickness of the boundary layer, where the decrease in heat exchange along the path of the annulus due to the increase in the boundary layer thickness.

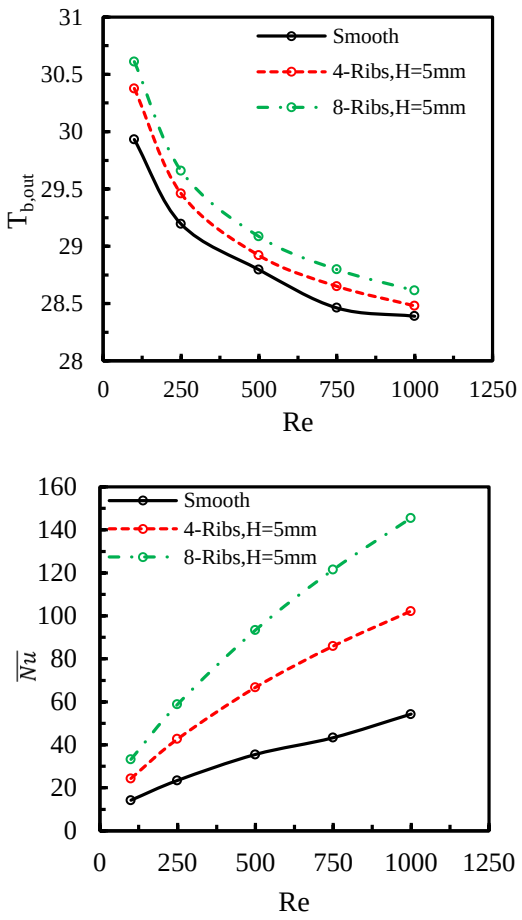

Figure 6. Numerical variation of (a) cold outlet temperature, and (b) average Nusselt number versus Reynolds numbers for ribbed as compared with smooth DPHE.

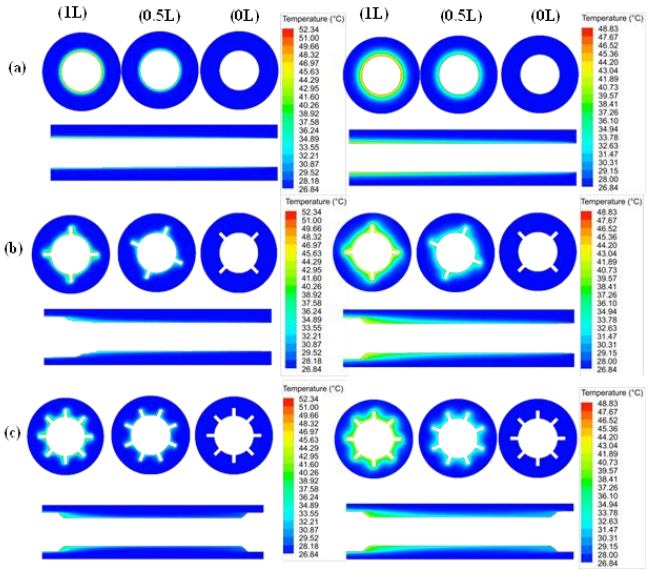

Figure 7. Temperature contours (left) at Re =1000 and (right) at Re = 100 at (a) smooth, (b) (4-ribs, H= 5 mm) and, (c) (8-ribs, H= 5 mm).

4.3. The effect of rib heights on hydraulic-thermal performance

4.3.1. Characteristics of fluid flow

The numerical data of friction factor (f) versus Reynolds numbers for two numbers of ribs (4 and 8-ribs) is shown in Fig. 8. The friction factor is inversely proportional with rising Reynolds numbers, the f increases with increasing height ribs of DPHE.

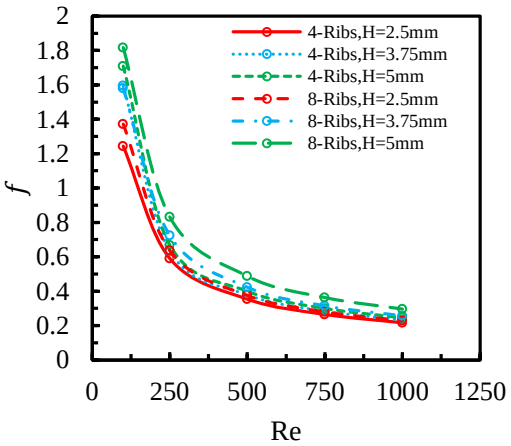

Figure 8. Variation of friction factor versus Reynolds numbers for two rib numbers and three different rib heights.

Fig. 9 displays contours of velocity field in the axial annular plane direction and the cross-sectional planes (at three different locations along the annulus) within the ribbed DPHE for two rib numbers (4 and 8-ribs) and two different rib heights (2.5 and 5 mm) at *Re* =100 and *Re* = 1000. When the fluid enters the annular space, the velocity distributes nearing from the ribs will be tilted at an angle of 45 degrees, and the velocity distribution begins to focus more and more along the path of the annulus gap, and this reason is due to the increase in the boundary layer thickness. Increasing the height of ribs leads to secondary flow in the annular gap and a decrease in the thickness of the hydraulic boundary layer. From the shape of the velocity distribution, the velocity at the entrance of the annular gap is uniform for all shapes, but at exit annulus, we notice that the velocity distribution in the center is higher than the velocity distribution near the surface of the pipe, and that is due to the effect of the increasing hydraulic boundary layer along the length of the pipe.

4.3.2. Heat transfer charactarestic

The averaged Nusselt number ($\overline{Nu}$) and outlet bulk fluid temperature ($T_{b,out}$) versus Reynolds numbers with two rib numbers (4 and 8-ribs) and three heights of ribs of DPHE are shown in Fig. 10. In general, the outlet bulk fluid temperature decreases with increasing Reynolds numbers and the greatest values of outlet fluid temperature occurs at 5 mm rib height. Moreover, the averaged Nusselt numbers increase with increasing values of Reynolds numbers. The highest values of Nusselt numbers take place at highest value of rib height (5 mm). The percentage of Nusselt number enhancement at *Re* =100 for three rib heights (H = 2.5, 3.75, 5 mm) and 4-ribs is (8%, 57%, 71%), respectively. While for 8-ribs of three rib heights (H= 2.5, 3.75 and 5 mm), the percentage of Nusselt number enhancement is (48%, 87%, 133%), respectively, compared with smooth DPHE.

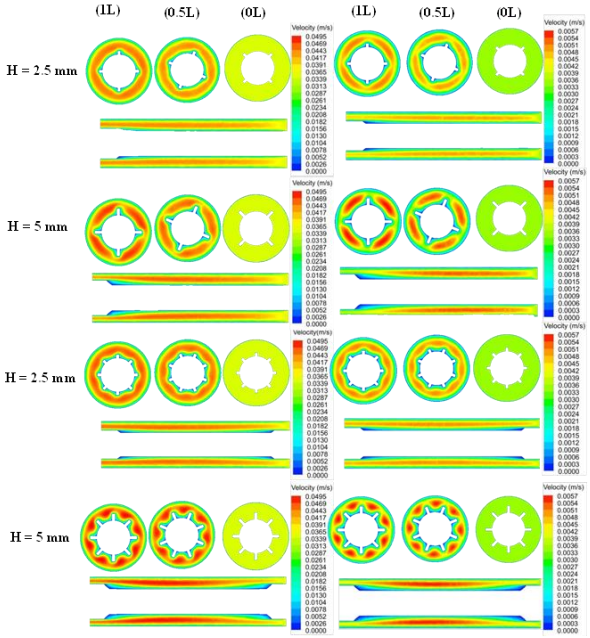

Figure 9. Velocity contours for ribbed double-pipeheatexchanger at Re =1000 (left) and Re = 100 (right) for two rib numbers (4-ribs and 8-ribs) and two different rib heights (2.5 mm and 5 mm).

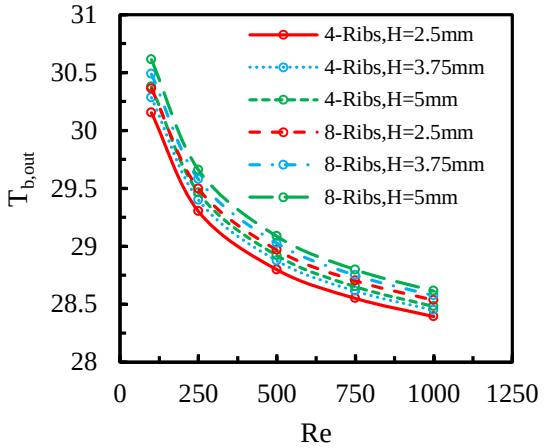

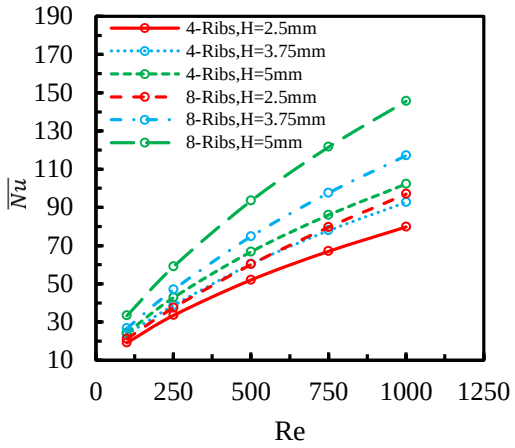

Figure 10. Numerical data for ribbed double pipe heat exchanger of (a) cold outlet bulk temperature, and (b) averaged Nusselt number versus Reynolds numbers.

Fig. 11 displays contours of temperature field in the axial annular plane direction and in the cross-sectional planes (at three different locations along the annulus) within the ribbed DPHE, with (H= 2.5 and 5 mm, W = 2mm) at *Re* = 100 and 1000. The insert helical ribs in the annulus path to generate secondary flows enhance fluid mixing between the hot surface of annular gap and the cold fluid in the mid of annulus, which lead to a high-temperature distribution. Increased height of helical ribs leads to increasing of surface area subjecting to convective heat transfer. The swirling flow is able to raise the rate of exchanged heat transfer. In (Fig .11-b and c) shows the heat exchange difference along the annulus , where heat transfer coefficient at the beginning of the annulus is high due to a decrease in the thickness of the boundary layer , where the decrease in heat transfer coefficient along the path of the annulus due to the increase in the boundary layer thickness.

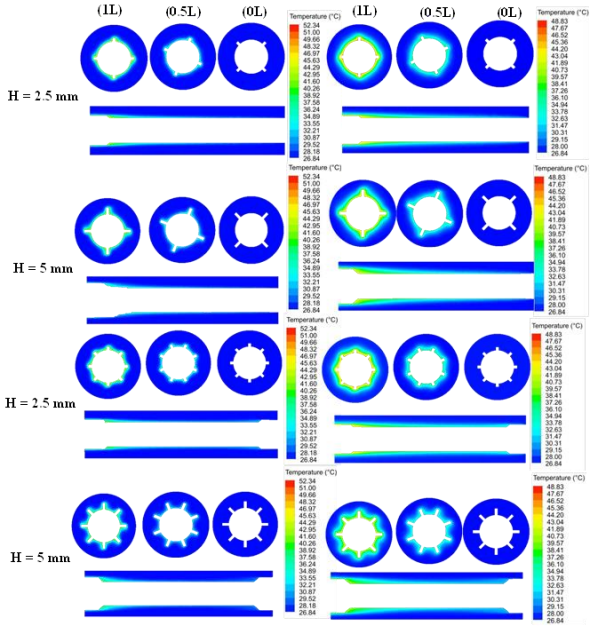

Figure 11. Temperature contours for ribbed double-pipe heat exchanger at Re =1000 (left) and Re = 100 (right) for two rib numbers (4-ribs and 8-ribs) and two different rib heights (2.5 and 5 mm).

4.4. Comprehensive performance analysis

The heat transfer enhancement is usually achieved at the expense of energy dissipated by extra friction; comparing the ribbed data results (Nusselt number and friction factor) to the reference case of a smooth DPHE is one way of studying the effect of ribs on the double-pipe heat exchanger performance. The performance evaluation criterion (PEC) versus Reynolds number is shown in Fig. 11 at three rib heights = (2.5, 3.75, 5 mm) and two numbers of ribs. The PEC gradually increases with increasing Reynolds numbers for all ribbed double-pipe heat exchangers due to the generated secondary flows and the thickness of thermal boundary layer. When the value of (*PEC*) is greater than one, this means that the amount of ($\overline{\boldsymbol{Nu}}_{,R}/\overline{\boldsymbol{Nu}}_{,S}$) is greater than of ($\boldsymbol{f}_{,R}/\boldsymbol{f}_{,S}$). The 8-ribs have the higher (*PEC*) as compared with 4-ribs double pipe heat exchanger. In addition, it is found that 8-ribs owns the highest performance over the Reynolds number range, and the top value of *PEC* is 2.40 at *Re* = 750, while for 4-ribs, the top value of ***PEC*** is 1.81 at *Re* = 750. The variation in the amount of ***PEC*** over the Reynolds number range is due to the variation of the averaged Nusselt number enhancement ratio and the friction factor ratio.

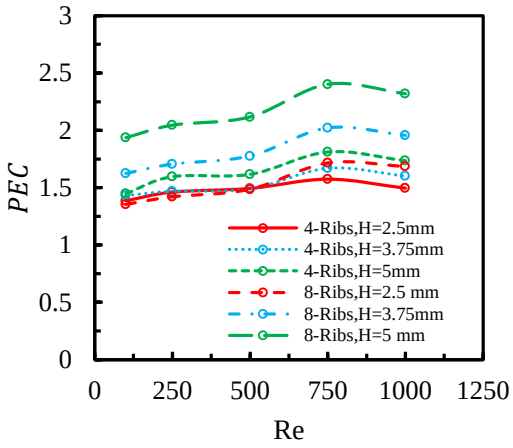

Figure 11: Showing the performance evaluation criteria for ribbed double-pipe heat exchanger with different rib heights.

5. Conclusion

A numerical model is employed to evaluate the hydraulic-thermal performance of a double-pipe heat exchanger with 45°-helical ribs. The impact of

numbers and heights of ribs are numerically examined. The flow of cold water in the annular gap was investigated in the range of Reynolds number from 100 to 1000 for achieving laminar flow regime. In general, the values of friction factor dramatically decrease with rising Reynolds numbers. The values of friction factor increase with increasing number of ribs of DPHE. However, the values of Nusselt number increase with increasing the number of ribs due to the reducing in the thermal boundary layer thickness. The percentage of averaged Nusselt number enhancement for three rib heights (H = 2.5, 3.75 and 5 mm) at 4-ribs is (34%, 65% and 71%), respectively. While for 8-ribs the enhancement percentage is (48%, 87% and 133%) as compared with the smooth double-pipe heat exchanger. In addition, the percentage of friction factor at (H = 2.5, 3.75 and 5 mm) and 4-ribs is (20%, 54% and 65%), while for 8-ribs it is (32%, 52% and 75%) at Re = 100. The percentage of friction factor increases with increasing in the number of ribs and rib heights compared with the smooth double-pipe heat exchanger.

References

[1] Mueller, A. C., "Heat exchangers, in Chapter 18 Handbook of Heat Transfer", W. M. Rohsenow and J. P. Hartnett, eds., McGraw-Hill, New York, 1973.

[2] Theodore L. Bergman, Adrienne S. Lavine, Frank P. Incropera, "Fundamentals of Heat and Mass Transfer", 7th Edition, John Wiley & Sons, Incorporated, 2011.

[3] SHAH, R. K. Classification of heat exchangers, in Heat Exchangers-Thermo-Hydraulic Fundamentals and Design. Kakac S., Bergles AE, Mayinger F., John Wily & Sons, NewYork, 1981.

[4] B. B. Verma and S. Kumar, "CFD Analysis and Optimization of Heat Transfer in Double Pipe Heat Exchanger with Helical-Tap Inserts at Annulus of Inner Pipe," vol. 13, no. 3, pp. 17–22, 2016.

[5] A. El Maakoul, A. Laknizi, S. Saadeddine, A. Ben Abdellah, M. Meziane, and M. El Metoui, "Numerical design and investigation of heat transfer enhancement and performance for an annulus with continuous helical baffles in a double-pipe heat exchanger," Energy Convers. Manag., vol. 133, pp. 76–86, 2017.

[6] A. El Maakoul, M. El Metoui, A. Ben Abdellah, S. Saadeddine, and M. Meziane, "Numerical investigation of thermohydraulic performance of air to water double-pipe heat exchanger with helical fins," Appl. Therm. Eng., vol. 127, pp. 127–139, 2017.

[7] M. T. Scholar and N. Kumar, "Heat Transfer Performance Analysis for Double Pipe Heat Exchanger Using Double Helical Tape Insert," IJIRST-International J. vol. 5, no. 3, pp. 1112–1118, 2019.

[8] J. R. Soni and J. B. Khunt, "CFD Analysis and Performance Evaluation of Concentric Tube in Tube Heat Exchanger," IJIRST-International J. Innov. Res. Sci. Technol., vol. 2, no. 1, pp. 18–21, 2015.

[9] Z. Zhang, D. Ma, X. Fang, and X. Gao, "Experimental and numerical heat transfer in a helically baffled heat exchanger combined with one three-dimensional finned tube," Chem. Eng. Process. Process Intensif., vol. 47, no. 9–10, pp. 1738–1743, 2008.

[10] P. Eiamsa-Ard, N. Piriyarungroj, C. Thianpong, and S. Eiamsa-Ard, "A case study on thermal performance assessment of a heat exchanger tube equipped with regularly-spaced twisted tapes as swirl generators," Case Stud. Therm. Eng., vol. 3, pp. 86–102, 2014.

[11] Pachegaonkar, Snehal S., Santosh G. Taji, and Narayan Sane. "Performance analysis of double pipe heat exchanger with annular twisted tape insert." International Journal of Engineering and Advanced Technology (IJEAT) 3.3 (2014): 402-406.

[12] S. Frank M. White "Fluid Mechanics" 8th edition 2008, Mc-Graw Hill Company, Phil. Mag., vol. 27. p. 77, 2009.

[13] F. M. White, 'Fluid Mechanics 8th in SI units', Journal of Visual Languages & Computing, vol. 11. p. 864, 2000.

[14] S. Eiamsa-ard and P. Promvonge, "Thermal characteristics of turbulent rib-grooved channel flows", Int. Commun. Heat Mass Transf., vol. 36, no. 7, pp. 705–711, 2009.

[15] R. K. Shah and A. L. London, "Concentric Annular Ducts," Laminar Flow Forced Convection Ducts, pp. 284–321, 1978.

Nomenclatures

L	Heat exchanger length (m)
A_c	Cross-section area (m^2)
D_{out}	Outer diameter of outer pipe (m)
D_{in}	inner diameter of outer pipe (m)
d_{out}	Outer diameter of inner pipe (m)
t	Thickness of inner pipe (m)
W	Width of rib(m)
H	Height of rib (m)
D_h	Hydraulic diameter (m)
p_t	Pitch of tape (m)
p_w	Pitch of wire (m)
p_c	Pitch of semi-circle disc (m)
w	Width of tape (m)
d_w	Diameter of wire (m)
$\bar{h}$	Average heat transfer coefficient ($W/m^2.℃$)
C_P	Specific heat (J/kg .°C)
k	Thermal conductivity (W/m .℃)
L	Length of channel (m)
$\dot{m}$	Mass flow rate (kg/s)
$\overline{Nu}$	Average Nusselt number
$\dot{m}$	Mass flow rate (kg/s)
N	Number of ribs
P	Pressure (Pa)
p	perimeter (m)
Q	Heat received (W)
Re	Reynolds number
T	Temperature (˚C)
T_b	Bulk fluid temperature (˚C)
T_s	Surface temperature (˚C)
U_m	Mean velocity (m/s)
p_r	Pitch of rib (m)
Greek Symbols	
μ	Dynamic viscosity
ρ	Density (kg/s)
ΔP	Pressure drop (pa)
θ	Inclined angle (°)
Subscripts	
f_c	Cold fluid domain
R	Ribbed surface
in	Inlet
out	Outlet
S	Straight surface